Journal of Power Sources 266 (2014) 471–474

Contents lists available at ScienceDirect

Journal of Power Sources

journal homepage: www.elsevier.com/locate/jpowsour

Short communication

High-rate charge/discharge properties of Li-ion battery using carbon-coated composites of graphites, vapor grown carbon fibers, and carbon nanohorns

Ryota Yuge*, Noriyuki Tamura, Takashi Manako, Kaichiro Nakano, Kentaro Nakahara

Smart Energy Research Laboratories, NEC Corporation, 34 Miyukigaoka, Tsukuba 305-8501, Japan

HIGHLIGHTS

- We succeeded in preparing the carbon-coated composites of graphites, VGCF, and CNHs.
- The quantity of coated carbon films was estimated as 4 wt% from the weight change of TGA.
- The carbon-coated composites achieved the excellent high-rate properties for half-cell.

ARTICLE INFO

Article history:
Received 28 August 2013
Received in revised form
12 April 2014
Accepted 13 May 2014
Available online 21 May 2014

Keywords:
Li ion battery
Quick charge–discharge
Carbon nanohorns
Carbon-coated composites

ABSTRACT

The mixture of graphite, vapor grown carbon fibers (VGCFs), and carbon nanohorns (CNHs) was heat-treated in Ar atmosphere and carbon-coated by using a chemical vapor deposition (CVD) method (C-graphite/VGCF/CNH). Scanning electron microscopy observation showed that graphite, VGCF, and CNHs were covered by carbon film. Thermogravimetric analysis also indicated that carbon film formed by the CVD method combusted at 550 °C and the quantity of carbon film was about 4 wt%. The C-rate properties of half-cell for C-graphite/VGCF/CNH were superior to those for the mixture of graphite, VGCF, and CNHs (C-graphite/VGCF/CNH (discharge) : 3C/0.1C, 85%, graphite/VGCF/CNH (discharge) : 3C/0.1C, 50%), accelerating a promising application for quick charge–discharge of Li-ion batteries.

1. Introduction

Lithium-ion batteries have been widely used for decades in portable electronic devices such as laptops and cellular phones [1–3] due to their large energy density and long life. Recently, their applications in electric vehicles (EV) and plugin hybrid electric vehicles (HEV) have been demanded, leading to increases in battery size and capacity [4,5]. Specifically, the demand for quicker charging of EVs has been increased drastically for very long charge time. Therefore, a Li-ion battery operating at high-rates needs to be developed to realize the above industrial applications [6–10].

To achieve the operation at high-rates, the internal resistances on anode electrodes need to be decreased. In general, their origins are mainly the contact resistances between active materials and/or active materials and conductive additives for charge and discharge with high energy density [11]. Therefore, decreasing them should help to improve the rate properties. Here, we tried to prepare novel composites of graphite, vapor grown carbon fibers (VGCFs), and carbon nanohorns (CNHs) covered by carbon films (C-graphite/VGCF/CNH). The VGCF [12] and CNHs [13–15] are applied as filler to enhance the electrical conductivity. The CNHs that have highly dispersive properties [16,17] are also expected to be packed closely in the empty space of graphites and VGCF and behave as a buffer for volume change in the graphite during charge–discharge. The carbon coating also needs to decrease the irreversible capacity and electronic resistance of anode [18,19]. We also thoroughly investigated the relationship between the structure of C-graphite/VGCF/CNH and electrochemical rate-properties.

2. Experimental

Graphite (MAG10) (Hitachi chemical Co., Ltd.) (Particle size: 10–20 μm) (1 g), vapor grown carbon fibers (VGCFs) (Showa denko K. K.) (Diameter: 150 nm) (20 mg), and carbon nanohorns (CNHs) (NEC corporation) (Particle size: 100 nm) (20 mg) were dispersed in ethanol (40 ml) and stirred at room temperature for about 10 min. The mixture was filtered, and black powder was obtained on the

* Corresponding author. Tel.: +81 29 850 1146; fax: +81 29 856 6137.
E-mail address: r-yuge@bk.jp.nec.com (R. Yuge).

http://dx.doi.org/10.1016/j.jpowsour.2014.05.068
0378-7753/

filter paper (graphite/VGCF/CNH). They were placed on an alumina boat located at the center of a reactor tube in an electric furnace and heated in the reactor at 1000 °C for three hours in Ar flowing at 300 ml min^{-1}. Then, the heating temperature was decreased to 800 °C for chemical vapor deposition (CVD) [20]. After the target temperature was reached, the gas flow was switched to C_2H_2 gas of a carbon feedstock, diluted in Ar, and kept for 30 min (C-graphite/VGCF/CNH). Finally, the reactor was cooled to room temperature in the Ar gas flow. The specific surface area of the graphite (MAG10), graphite/VGCF/CNH, and C-graphite/VGCF/CNH was estimated as 40, 150, and 450 m^2 g^{-1}, respectively.

The structures of the specimens were observed with a scanning electron microscope (SEM) (Hitachi S-4800). The SEM was operated at 1.0 kV. The thermogravimetric analysis (TGA) (BRUKER AXS TG-DTA2000SA) was performed in an oxygen atmosphere at temperatures ranging from room temperature to 900 °C. The TGA was carried out at a ramp rate of 10 °C min^{-1}. A constant amount (ca. 1.5 mg) of sample was used for TGA.

A coin-type electrochemical cell (2320) that has a lithium metal counter electrode and 1 M $LiPF_6$/EC + DEC electrolyte (UBE Kosan Co., Ltd., EC: DEC = 3:7 (volume), water content = 10 ppm) was prepared for charge–discharge measurements. Anode electrode was prepared from a mixture of C-graphite/VGCF/CNH and polyvinylidene fluoride (PVDF) binder. The ratio of the binder was 5 wt% in the anode electrode. The loading of active materials was 6–7 mg cm^{-2}. Galvanostatic charge (lithiation)/discharge (delithiation) measurements were carried out in the range of 0–0.8 or 2.5 V in a thermostatic chamber controlled at 20 °C (Electrofield Battery Labo system).

First, to determine the capacities of the samples, the cells were charged to 0 V at the constant current (CC) mode at 0.1 mA cm^{-2}. Then, the cells were discharged in the range of 0–2.0 V at the CC mode of 0.1 mA cm^{-2}. The charge and discharge rate performance was measured in the range of 0.1C–3C. For the charge rate performance, the anode was firstly discharged to 0.8 V at the constant current constant voltage (CCCV) mode and then charged to 0 V at CC mode of 0.1–3C. For the discharge rate performance, the anode was firstly charged to 0 V at the CCCV mode and then discharged to 0.8 V at CC mode of 0.1–3C.

Electrochemical impedance measurements (Solartorn 2010) were carried out using coin cell at a charging state after initial charge–discharge. The explored frequency range was from 100 kHz to 1 mHz under 10 mV of amplitude and no bias voltage was applied.

3. Results and discussion

3.1. Structural characterization

Fig. 1 shows typical SEM images of graphite/VGCF/CNH (a, b, and c) and C-graphite/VGCF/CNH (d, e, and f). The graphite and CNHs were spherical structures with the sizes of about several micrometers and one hundred nano-meters in diameter, respectively. The well-known VGCF had a tube structure of 10–100 μm in length and diameter of about 150 nm. As shown in Fig. 1e and f, the graphite and/or VGCF in C-graphite/VGCF/CNH had a smoother and rounder surface structure than those of graphite/VGCF/CNH. Very small particles were also deposited on graphite and VGCF surfaces. Therefore, each of graphite, VGCF, and CNHs was covered and attached by thin carbon layers.

Fig. 2 (a) shows the weight-temperature curves in O_2 atmosphere obtained from the TGA. Fig. 2 (b) shows the derivative curves of the weight-decrease to temperature, where main peak appears at about 600 °C for CNHs, 780 °C for VGCF, 790 °C for graphite/VGCF/CNH and C-graphite/VGCF/CNH, and 800 °C for graphite. The main peaks of derivative curves of graphite/VGCF/CNH and C-graphite/VGCF/CNH were almost the same, indicating the no drastic change of graphite, VGCF, and CNH themselves by CVD process. The broad peak at the range from 520 to 640 °C for C-graphite/VGCF/CNH is attributed to carbon layers prepared by the CVD method. The quantity of the coated carbon films was estimated as 4wt% from the weight change (in set in Fig. 2(b)). The peaks at 680–720 °C of CNHs are attributed to micrometer-sized graphitic impurities formed intrinsically from the graphite target by CO_2 laser ablation [21].

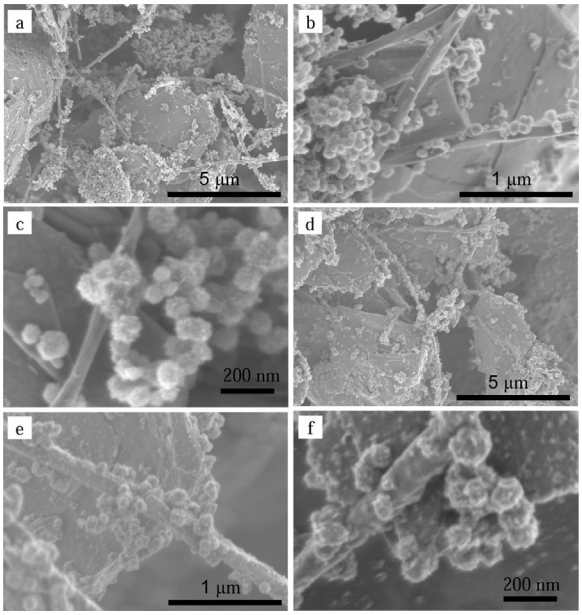

Fig. 1. SEM images of graphite/VGCF/CNH (a b, and c) and C-graphite/VGCF/CNH (d, e, and f).

3.2. Charge–discharge properties

Fig. 3 shows the first charge–discharge curves of the Li-ion cell prepared with the graphite, graphite/VGCF/CNH and C-graphite/VGCF/CNH electrode in the range of 0–2.5 V. The graphite in Fig. 3

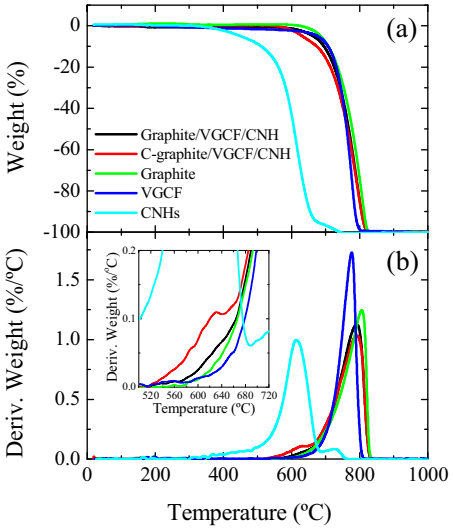

Fig. 2. TGA and derivative TGA of graphite/VGCF/CNH and C-graphite/VGCF/CNH.

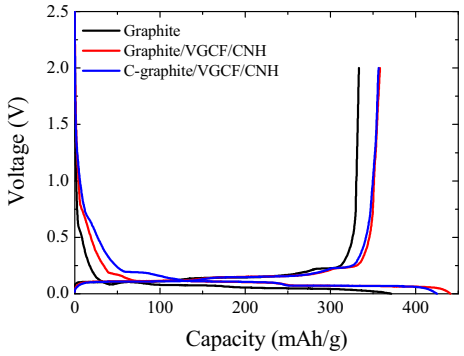

Fig. 3. Charge-discharge curves of graphite, graphite/VGCF/CNH, and C-graphite/VGCF/CNH.

shows the electrode without conductive additive. The cells performance exhibited an irreversible capacity loss during the first cycle, which is typical for carbon-based anode materials and explained by the formation of solid electrolyte interface (SEI) and/or irreversible reaction of surface functional groups [22]. The charge capacity, discharge capacity and columbic efficiency for graphite, graphite/VGCF/CNH, and C-graphite/VGCF/CNH were 371 mAh g^{-1}, 333 mAh g^{-1}, 90%, 440 mAh g^{-1}, 358 mAh g^{-1}, 81%, and 424 mAh g^{-1}, 356 mAh g^{-1}, 84%, respectively. These results indicated that the irreversible capacities of C-graphite/VGCF/CNH and graphite/VGCF/CNH were almost the same although specific surface area of C-graphite/VGCF/CNH was larger than that of graphite/VGCF/CNH. Therefore, we considered that the SEI on C-graphite/VGCF/CNH was formed thinly by the initial charge. The irreversible capacity originated from the decomposition of electrolyte relates strongly to the specific surface area and active sites such as edges and/or defects. The decomposition of electrolyte was suppressed for small active sites of the carbon film on C-graphite/VGCF/CNH. Here, the capacity was calculated from the weight of electrode materials not including the binder weight, VGCF, CNHs and carbon films. These initial capacities were close to the theoretical reaction of the first lithium insertion of graphite.

Fig. 4 shows the charge rate characteristics of C-graphite/VGCF/CNH and graphite/VGCF/CNH. Each capacity gradually decreased with the increase of the rate. The decrease quantity of capacity for each rate of C-graphite/VGCF/CNH was much smaller than that of graphite/VGCF/CNH. We considered that the contact resistance between graphite, VGCF, and CNHs decreased by carbon-carting. As a result, the internal resistance of C-graphite/VGCF/CNH electrode decreased, which achieved good rate properties. It should be noted that the influence of Li diffusion velocity in the active materials and/or electrodes possibly becomes dominant for high rates such as 2–3C to decrease drastically.

Fig. 5 shows the discharge rate characteristics of C-graphite/VGCF/CNH and graphite/VGCF/CNH. The C-graphite/VGCF/CNH shows about 340–350 mAh g^{-1} at the rate from 0.1 to 1C, while graphite/VGCF/CNH shows the gradual decrease of discharge capacity with the increase of the rate. This is because the decrease of the internal resistance of C-graphite/VGCF/CNH electrode was carried out by the carbon coating. These results indicate that C-graphite/VGCF/CNH is a suitable anode material for a high-power battery.

Fig. 6 shows typical impedance spectra of C-graphite/VGCF/CNH and graphite/VGCF/CNH. The impedance was measured at a charging state after initial charge–discharge. The impedance spectra exhibit two semicircles and a straight line with the decrease of frequency in the range from 100 kHz to 10 mHz. Since the cathode electrode and electrolyte solution were exactly the same,

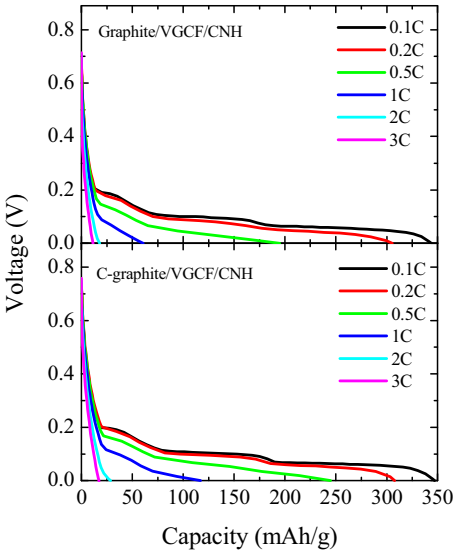

Fig. 4. Comparison of the charge rate characteristics of C-graphite/VGCF/CNH and graphite/VGCF/CNH.

the difference in the impedance are made by the anode electrode. The origin of the two semicircles can be interpreted as follows. The first can be assigned mainly to the SEI film and the contact resistance between active materials and/or active materials and a conductive additive [10,23]. The diameter of the first semicircle for the C-graphite/VGCF/CNH electrode was much smaller than that for the graphite/VGCF/CNH electrode even if the curves originated to the SEI film and the contact resistance overlapped. The second can be assigned to the charge transfer resistance related to the lithium intercalation process [10,23]. The linear portion is attributed to diffusion resistance of Li-ion in electrodes. These results indicated that the internal resistance and SEI resistance of C-graphite/VGCF/CNH electrode were smaller than those of the graphite/VGCF/CNH electrode.

We discuss why the contact resistance of the C-graphite/VGCF/CNH electrode decreased. The heat-treatment at 1000 °C in Ar caused the increase in crystallinity due to the restoration of a

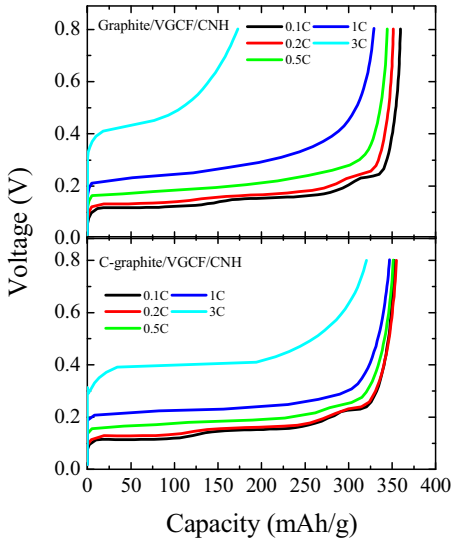

Fig. 5. Comparison of the discharge rate characteristics of C-graphite/VGCF/CNH and graphite/VGCF/CNH.

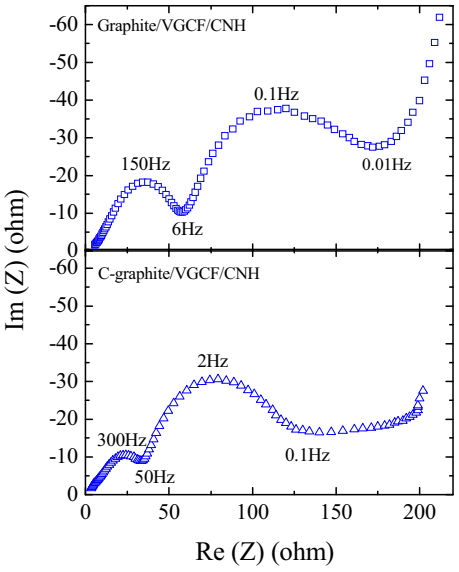

Fig. 6. Impedance spectra of C-graphite/VGCF/CNH and graphite/VGCF/CNH after charging.

defective site of graphite, VGCF, and CNHs [24–26]. This effect did not contribute drastically to the combustion reaction in O_2 by TGA because the increase in crystallinity was mostly due to the restoration of the defects on the surface. The good conduction passway through graphite, VGCF, and CNHs was formed by carbon-coating. After all, we can conclude that the high rate performance was achieved by unifying graphite, VGCF, and CNHs.

4. Conclusion

In this study, we succeed in preparing novel composites of graphite, VGCF, and CNHs by heat-treatment at 1000 °C in Ar and carbon-coating using a chemical vapor deposition (CVD) method at 800 °C in C_2H_2/Ar. The obtained samples, C-graphite/VGCF/CNH, were fixed and unified by carbon film. The C-rate properties of a half-cell for a C-graphite/VGCF/CNH electrode were superior to those of the mixture of graphite, VGCF, and CNH, (C-graphite/VGCF/CNH (discharge): 3C/0.1C, 85%, graphite/VGCF/CNH (discharge): 3C/0.1C, 50%). This is because the internal resistance of C-graphite/VGCF/CNH was decreased by the carbon coating. We believe that these composites are promising for quick charge–discharge of Li-ion batteries.

References

[1] M. Endo, C. Kim, K. Nishimura, T. Fujino, K. Miyashita, Carbon 38 (2000) 183–197.
[2] E.A. Cuellar, M.E. Manna, R.D. Wise, A.B. Gavrilov, M.J. Bastian, R.M. Brey, J. DeMatteis, J. Power Sources 96 (2001) 184–198.
[3] U. Köhler, J. Kümpers, M. Ullrich, J. Power Sources 105 (2002) 139–144.
[4] Y.E. Hyung, S.I. Moon, D.H. Yum, S.K. Yun, J. Power Sources 81–82 (1999) 842–846.
[5] T. Horiba, K. Hironaka, T. Matsumura, T. Kai, M. Koseki, Y. Muranaka, J. Power Sources 97–98 (2001) 719–721.
[6] H. Fujimoto, J. Power Sources 195 (2010) 5019–5024.
[7] R. Krishnan, T.M. Lu, N. Koratkar, Nano Lett. 11 (2011) 377–384.
[8] R. Mukherjee, A.V. Thomas, A. Krishnamurthy, N. Koratkar, ACS Nano 6 (2012) 7867–7878.
[9] T.S. Yeh, Y.S. Wu, Y.H. Lee, Mater. Chem. Phys. 130 (2011) 309–315.
[10] R. Song, H. Song, J. Zhou, X. Chen, B. Wu, H.Y. Yang, J. Mater. Chem. 22 (2012) 12369–12374.
[11] G. Liu, H. Zheng, A.S. Simens, A.M. Minor, X. Song, V.S. Battaglia, J. Electrochem. Soc. 154 (2007) A1129–A1134.
[12] M. Endo, Y.A. Kim, T. Hayashi, K. Nishimura, T. Matusita, K. Miyashita, M.S. Dresselhaus, Carbon 39 (2001) 1287–1297.
[13] S. Iijima, M. Yudasaka, R. Yamada, S. Bandow, K. Suenaga, F. Kokai, K. Takahashi, Chem. Phys. Lett. 309 (1999) 165–170.
[14] N. Li, Z. Wang, K. Zhao, Z. Shi, Z. Gu, S. Xu, Carbon 48 (2010) 1580–1585.
[15] K. Urita, S. Seki, S. Utsumi, D. Noguchi, H. Kanoh, H. Tanaka, Y. Hattori, Y. Ochiai, N. Aoki, M. Yudasaka, S. Iijima, K. Kaneko, Nano Lett. 6 (2006) 1325–1328.
[16] R. Yuge, J. Miyawaki, T. Ichihashi, S. Kuroshima, T. Yoshitake, T. Ohkawa, Y. Aoki, S. Iijima, M. Yudasaka, ACS Nano 4 (2010) 7337–7343.
[17] R. Yuge, M. Yudasaka, K. Yoyama, T. Yamaguchi, S. Iijima, T. Manako, Carbon 50 (2012) 1925–1933.
[18] M. Yoshio, H. Wang, K. Fukuda, Y. Hara, Y. Adachic, J. Electrochem. Soc. 147 (2000) 1245–1250.
[19] H. Wang, M. Yoshio, T. Abe, Z. Ogumi, J. Electrochem. Soc. 149 (2002) A499–A503.
[20] S. Maruyama, R. kojima, Y. Miyauchi, S. Chiashi, M. Kohno, Chem. Phys. Lett. 360 (2002) 229–234.
[21] J. Fan, M. Yudasaka, D. Kasuya, T. Azami, R. Yuge, H. Imai, Y. Kubo, S. Iijima, J. Phys. Chem. B 109 (2005) 10756–10759.
[22] P. Verma, P. Maire, P. Novák, Electrochim. Acta 55 (2010) 6332–6341.
[23] J. Guo, A. Sun, X. Chen, C. Wang, A. Manivannan, Electrochim. Acta 56 (2011) 3981–3987.
[24] F.G. Emmerich, Carbon 33 (1995) 1709–1715.
[25] M. Endo, K. Nishimura, Y.A. Kim, K. Hakamada, T. Matushita, M.S. Dresselhaus, G. Dresselhaus, J. Mater. Res. 14 (1999) 4474–4477.
[26] M. Yudasaka, T. Ichihashi, D. Kasuya, H. Kataura, S. Iijima, Carbon 41 (2003) 1273–1280.